Dicke superradiance of a two-component Fermi gas coupled to a quantized light field

Ming-Yue Yang,[1] Hong-Hao Yin,[1] Lin Wen,[2] An-Chun Ji,[1] and Qing Sun[1,*]
[1]*Department of Physics, Capital Normal University, Beijing 100048, China*
[2]*College of Physics and Electronic Engineering, Chongqing Normal University, Chongqing 401331, China*

(Received 24 June 2021; revised 21 September 2021; accepted 28 October 2021; published 12 November 2021)

We study the superradiance transition of a two-component three-dimensional Fermi gas interacting with a single-mode light field of Dicke-type coupling. We find that for a noninteracting gas, due to the Fermi blocking, a unique superradiant state with a superradiant outer shell surrounding an inner Fermi sea may appear, and the critical atom-light coupling strength g_c to trigger the superradiance approaches $\sqrt{\omega_c E_F/3}$ even for a vanishing transition frequency between a two-spin state ($\omega_a \to 0$), in contrast to $g_c \sim \sqrt{\omega_c \omega_a} \to 0$ for a bosonic or spin system. When the atom-atom attraction is included, we find that the atomic superfluid would compete with the superradiance directly and both orders cannot coexist, giving rise to an interesting ground-state phase diagram with a tricritical point. The resultant phases and phase transitions are characterized by the unique fluctuation spectrum beyond the mean-field level. We further analyze the effects caused by the decay of the light field, which is inevitable for a possible realization in a cavity with a cold atom system. Our results would be beneficial for the understanding of the interplay between Fermi superfluid and superradiance.

DOI: 10.1103/PhysRevA.104.053313

I. INTRODUCTION

In recent years, the dynamical realization [1] of the well-known Dicke superradiance [2–5] in a cavity with Bose-Einstein condensates [6,7] has stimulated intensive research to study the nontrivial effects in atom-cavity systems brought about by collective atom-light coupling [8–27]. Such effects include the superradiant enhancement of a Fermi gas with a nested Fermi surface [11–13] or a disordered Bose-Einstein condensate (BEC) [15–18], the induced long-range interactions between atoms [19,20], and the multimode superradiance with emergent U(1) symmetry [21–23]. Nevertheless, in most of these works the external motion degrees of freedom (DOFs) of the atom are used to mimic the two levels in the Dicke model, and the superradiance transition with internal states in the cavity setup [28] has only been realized recently [29,30].

The inclusion of the internal DOFs can have profound effects on the superradiance transition as well as the many-body behaviors of the underlying systems [31–50]. For example, it may lead to the self-organized spin texture in a spinor BEC [31], the unconventional pairing of Fermi gas [35–37], and the cavity-assisted dynamical spin-orbit coupling [38–48]. Compared to the well-established Dicke superradiance of a bosonic or spin system, there are few works devoted to fermionic assemblies [51–54], and it is still unclear how the ground state of a three-dimensional spinful Fermi gas with internal atom-light coupling is affected by the superradiance and vice versa.

In this paper, we address this issue by studying the ground state and excitation spectrum of a two-component three-dimensional Fermi gas coupled to a quantized light field homogeneously. We find that the ground state of the Fermi gas is strongly affected by the atom-light coupling with unique features. The main results are as follows: (i) In the presence of a Fermi surface of a noninteracting gas, finite atom-light coupling $g_c \sim \sqrt{\omega_c E_F/3}$ is needed to drive a superradiant transition for a vanishing atomic transition frequency, in contrast to $g_c \sim \sqrt{\omega_c \omega_a} \to 0$ of a usual bosonic or spin system. Meanwhile, a superradiant state may appear that involves only a partial section of the outer atoms, with the remaining atoms forming an inner Fermi sea; this is referred to as phase separation of the superradiance and normal gas in momentum space. (ii) When the atomic attraction is included, as the atom-light coupling behaves as an effective transverse magnetic field, the Fermi superfluid from the singlet pairing would compete with the superradiance order directly, giving rise to a first-order transition between these two states in the ground-state phase diagram with a tricritical point even for a vanishing atomic polarization. (iii) The observable excitation spectrum beyond the mean-field level is obtained to characterize the resultant phases and phase transitions. A further analysis shows that a finite decay of the light field would shift the phase boundary by renormalizing the superradiance threshold and lead to a finite lifetime of the excitations, which are closely relevant in experiment. This work would be helpful in the search for nontrivial many-body hybrid states of atoms and light.

The rest of this paper is organized as follows: In Sec. II, we present the model and derive the mean-field self-consistent equations with the path integral approach. In Sec. III A, we first analyze the superradiance transition of an ideal Fermi gas, where the critical coupling can be determined analytically. Then we determine the ground-state phase diagram numerically for an interacting gas in Sec. III B, and we discuss the interplay of Fermi superfluid and superradiance. In Sec. III C,

*sunqing@cnu.edu.cn

we derive the excitation spectrum of the Gaussian fluctuation around the mean-field ground state, which can characterize the unique features of the diverse phases and phase transitions. Finally, in Sec. IV, we discuss the experiment-related dissipation effect caused by the decay of the light field on the superradiant transition as well as the excitation spectrum, and we conclude in the end.

II. THE MODEL AND FORMULISM

Let us consider a three-dimensional two-component (labeled as $\sigma = \uparrow, \downarrow$) Fermi gas of mass m interacting with a single-mode light field homogeneously through a Dicke-type coupling, the Hamiltonian of which can be written as (by setting $\hbar = 1$)

$$H = \omega_c \hat{a}^\dagger \hat{a} + \frac{g(\hat{a}^\dagger + \hat{a})}{\sqrt{N}} \int d\mathbf{r}[\hat{\psi}_\uparrow^\dagger(\mathbf{r})\hat{\psi}_\downarrow(\mathbf{r}) + \hat{\psi}_\downarrow^\dagger(\mathbf{r})\hat{\psi}_\uparrow(\mathbf{r})] + \int d\mathbf{r}\Big[\sum_\sigma \hat{\psi}_\sigma^\dagger(\mathbf{r})\Big(-\frac{\nabla^2}{2m} - \mu_\sigma\Big)\hat{\psi}_\sigma(\mathbf{r}) + \frac{U}{2}\hat{n}(\mathbf{r})^2\Big], \tag{1}$$

where $\hat{a}$ and $\hat{\psi}_\sigma$ represent the annihilation operators of the photon and atom of spin σ, respectively. ω_c is the frequency of the light field, and we have assumed a homogeneous atom-light interaction with the single-photon coupling strength g. The state-dependent chemical potentials are $\mu_\uparrow = \mu - \frac{\omega_a}{2}$ and $\mu_\downarrow = \mu + \frac{\omega_a}{2}$, with μ the chemical potential to fix the total atom number N, and ω_a the transition frequency between two spin states playing as a Zeeman field. At low temperatures, the atomic interaction is well described by the contact density-density attraction with strength $U(<0)$, which connects to the low-energy s-wave scattering length a_s via the renormalization relation $\frac{m}{4\pi a_s} = \frac{1}{U} + \frac{1}{V}\sum_{\mathbf{k}} \frac{1}{2\varepsilon_{\mathbf{k}}}$. Here the atomic density is $\hat{n} \equiv \hat{n}_\uparrow + \hat{n}_\downarrow$ with $\hat{n}_\sigma = \hat{\psi}_\sigma^\dagger \hat{\psi}_\sigma$, $\varepsilon_{\mathbf{k}} = \mathbf{k}^2/2m$ with $\mathbf{k}$ the momentum of atom, and V is the quantum volume.

Hamiltonian (1) bears the symmetry of $U(1) \otimes Z_2$, indicating that the total atom number $\hat{N} = \int d\mathbf{r}\, \hat{n}(\mathbf{r})$ and the parity $\hat{P} \equiv \exp\{i\pi(\hat{a}^\dagger \hat{a} + \hat{N})\}$ are conserved. In general, one can obtain the superfluid or superradiance order from the spontaneous breaking of $U(1)$ or Z_2 symmetry, respectively. When both orders are treated on an equal footing, they would interplay with each other and give rise to rich physics discussed in the following.

We aim to study the mean-field ground state and fluctuation spectrum of Hamiltonian (1). To this end, it is convenient to work in the frame of a path integral by writing the partition function as $Z = \int D[\bar{\psi}, \psi, \bar{\alpha}, \alpha] \exp(-S[\bar{\psi}, \psi, \bar{\alpha}, \alpha])$ [55], where ψ_σ and α represent the Grassmann field and boson field variables of fermion and photon, and the action

$$S = \int_0^\beta d\tau \int d\mathbf{r}\Big[\sum_\sigma \bar{\psi}_\sigma \partial_\tau \psi_\sigma + H\Big] + \int_0^\beta d\tau\, \bar{\alpha}\partial_\tau \alpha. \tag{2}$$

Here $\beta \equiv \frac{1}{k_B T}$, with k_B the Boltzmann constant and T the temperature.

By introducing the pairing field $\Delta(\mathbf{r}, \tau) = U\psi_\downarrow(\mathbf{r}, \tau)\psi_\uparrow(\mathbf{r}, \tau)$ to decouple the atomic interaction and making use of the Nambu representation $\bar{\Psi}(\mathbf{r}, \tau) = (\bar{\psi}_\uparrow\ \bar{\psi}_\downarrow\ \psi_\uparrow\ \psi_\downarrow)$, the action after the standard Hubbard-Stratonovich transformation can be recast as

$$S = \int d\tau\, d\mathbf{r}\Big[\frac{1}{2}\bar{\Psi}\mathcal{G}^{-1}\Psi - \frac{|\Delta(\mathbf{r}, \tau)|^2}{U} + \frac{(\hat{K}_\uparrow + \hat{K}_\downarrow)}{2}\Big] + \int d\tau\, \bar{\alpha}(\omega_c + \partial_\tau)\alpha, \tag{3}$$

where $\hat{K}_\sigma = -\frac{\nabla^2}{2m} - \mu_\sigma$, and $\mathcal{G}$ is the single-particle Green's function with the inverse

$$\mathcal{G}^{-1} = \begin{pmatrix} \partial_\tau + \hat{K}_\uparrow & \frac{g(\bar{\alpha}+\alpha)}{\sqrt{N}} & 0 & \Delta \\ \frac{g(\bar{\alpha}+\alpha)}{\sqrt{N}} & \partial_\tau + \hat{K}_\downarrow & -\Delta & 0 \\ 0 & -\bar{\Delta} & \partial_\tau - \hat{K}_\uparrow & -\frac{g(\bar{\alpha}+\alpha)}{\sqrt{N}} \\ \bar{\Delta} & 0 & -\frac{g(\bar{\alpha}+\alpha)}{\sqrt{N}} & \partial_\tau - \hat{K}_\downarrow \end{pmatrix}. \tag{4}$$

Integrating out the field Ψ, we arrive at the effective action

$$S_{\text{eff}} = \int d\tau\, d\mathbf{r}\Big[-\frac{1}{2\beta}\ln(-\beta\mathcal{G}^{-1}) - \frac{|\Delta(\mathbf{r}, \tau)|^2}{U} + \frac{1}{2}(\hat{K}_\uparrow + \hat{K}_\downarrow)\Big] + \int d\tau\, \bar{\alpha}(\omega_c + \partial_\tau)\alpha. \tag{5}$$

Here we have used the identity $\ln\det(\cdots) = \mathrm{Tr}\ln(\cdots)$.

In what follows, we write $\Delta = \Delta_0 + \delta\Delta$ and $\alpha = \alpha_0 + \delta\alpha$, with $\delta\Delta$ and $\delta\alpha$ being the fluctuations around the saddle point (Δ_0, α_0), and further we write $\mathcal{G}^{-1} = \mathcal{G}_0^{-1} + \mathcal{M}_{\text{F}}$ with $\mathcal{G}_0^{-1} = \mathcal{G}^{-1}|_{\Delta=\Delta_0, \alpha=\alpha_0}$ and

$$\mathcal{M}_{\text{F}} = \begin{pmatrix} \frac{g(\delta\bar{\alpha}+\delta\alpha)}{\sqrt{N}}\sigma_x & i\delta\Delta\sigma_y \\ -i\delta\bar{\Delta}\sigma_y & -\frac{g(\delta\bar{\alpha}+\delta\alpha)}{\sqrt{N}}\sigma_x \end{pmatrix}, \tag{6}$$

with σ_x and σ_y being the Pauli matrices. For small fluctuations, we expand the effective action (5) to the second order of $\mathcal{M}_{\text{F}}$ as $S_{\text{eff}} \simeq S_0 + S_{\text{F}}$, where

$$S_0 = \int d\tau\, d\mathbf{r}\Big[-\frac{1}{2\beta}\ln(-\beta\mathcal{G}_0^{-1}) - \frac{|\Delta_0|^2}{U} - \frac{\nabla^2}{2m} - \mu\Big] + \beta\omega_c|\alpha_0|^2 \tag{7}$$

and

$$S_{\text{F}} = \int d\tau\, d\mathbf{r}\Big[-\frac{|\delta\Delta|^2}{U} + \frac{1}{4\beta}(\mathcal{G}_0\mathcal{M}_{\text{F}})^2\Big] + \int d\tau\, \delta\bar{\alpha}(\partial_\tau + \omega_c)\delta\alpha \tag{8}$$

are the action at the saddle point and that of the fluctuation.

The mean-field ground state is generally determined by the thermodynamic potential at the saddle point $\Omega_0 \equiv \frac{1}{\beta}S_0$, which in terms of the momentum-frequency coordinates $(\mathbf{k}, i\omega_n)$ is given by

$$\Omega_0 = -\frac{1}{2\beta}\sum_{\mathbf{k}n,s}\ln\beta(i\omega_n - E_{\mathbf{k},s}) + \sum_{\mathbf{k}}\xi_{\mathbf{k}} + \omega_c|\alpha_0|^2 - \frac{V|\Delta_0|^2}{U}, \tag{9}$$

where $\omega_n = (n + \frac{1}{2})\frac{2\pi}{\beta}$, $n \in Z$ is the fermionic Matsubara frequency. $E_{\mathbf{k},s=\pm} = \sqrt{\xi_{\mathbf{k}}^2 + |\Delta_0|^2} \pm \sqrt{\omega_a^2/4 + g^2(\bar{\alpha}_0 + \alpha_0)^2/N}$

are the mean-field quasiparticle spectra in the presence of both superfluid order Δ and superradiance order α with $\xi_{\mathbf{k}} = \varepsilon_{\mathbf{k}} - \mu$. Further summing over the Matsubara frequency, we arrive at

$$\Omega_0 = -\frac{1}{\beta}\sum_{\mathbf{k},s}\ln(1+e^{-\beta E_{\mathbf{k},s}}) - \frac{V|\Delta_0|^2}{U} + \omega_c|\alpha_0|^2 + \sum_{\mathbf{k}}\left[\xi_{\mathbf{k}} - \frac{1}{2}(E_{\mathbf{k},+} + E_{\mathbf{k},-})\right]. \tag{10}$$

Finally, we minimize the above Ω_0 with respect to Δ_0 and α_0 to obtain the equations for the superfluid and superradiance, which are

$$-\frac{m}{4\pi a_s} = \frac{1}{V}\sum_{\mathbf{k}}\left[\sum_s \frac{1}{4\mathcal{E}_{\mathbf{k}}}\tanh\left(\frac{\beta E_{\mathbf{k},s}}{2}\right) - \frac{1}{2\varepsilon_{\mathbf{k}}}\right] \tag{11}$$

$$\omega_c = -\frac{1}{N}\sum_{\mathbf{k},s}\frac{sg^2}{\Lambda}\tanh\left(\frac{\beta E_{\mathbf{k},s}}{2}\right). \tag{12}$$

Here, $\mathcal{E}_{\mathbf{k}} = \sqrt{\xi_{\mathbf{k}}^2 + |\Delta_0|^2}$ and $\Lambda = \sqrt{\omega_a^2/4 + g^2(\bar{\alpha}_0 + \alpha_0)^2/N}$. Self-consistently solving the above Eqs. (11) and (12) together with the atomic number equation

$$N \equiv -\frac{\partial\Omega_0}{\partial\mu} = \sum_{\mathbf{k}}\left[1 - \sum_s \frac{\xi_{\mathbf{k}}}{2\mathcal{E}_{\mathbf{k}}}\tanh\left(\frac{\beta E_{\mathbf{k},s}}{2}\right)\right], \tag{13}$$

we can determine the ground state of the system. In this paper, we focus on the zero-temperature case, and the extension to finite temperature is straightforward.

III. SUPERRADIANCE TRANSITION OF THE FERMI GAS

A. Noninteracting case

We first consider the superradiance transition of a noninteracting gas. In this case, the superfluid is absent, and the self-consistent equations for the superradiance order (12) and atom number (13) at $T = 0$ reduce to

$$\omega_c = \frac{Vg^2}{3\pi^2 N\Lambda}[(\mu+\Lambda)^{3/2} - (\mu-\Lambda)^{3/2}], \tag{14}$$

$$\frac{N}{V} = \frac{1}{6\pi^2}[(\mu+\Lambda)^{3/2} + (\mu-\Lambda)^{3/2}]. \tag{15}$$

Then we can derive the critical coupling strength of superradiance,

$$g_c/E_F = \sqrt{\frac{4\omega_c E_F}{\omega_a^2 + 12\mu(\omega_a)^2}}, \tag{16}$$

where E_F is the Fermi energy and $\mu(\omega_a)$ can be obtained from Eq. (15) by setting $\alpha = 0$. In Fig. 1(a), we give the evolution of critical g_c with respect to the transition frequency ω_a (solid line). Across g_c, the system transits from a normal gas (NG) with $|\alpha| = 0$ to a superradiant state (SR) with $|\alpha| > 0$. Compared to the Dicke transition of a Bose or spin system where $g_c \simeq \sqrt{\omega_c\omega_a}$, the dependence of g_c on ω_a of the Fermi gas is quite different due to the Fermi blocking especially for $\omega_a \ll E_F$, where we have $\mu \simeq \sqrt{1 - \frac{3\omega_a^2}{32E_F^2}}$ and $g_c \simeq g_{c0}(1 - \frac{\omega_a^2}{192E_F^2})$. Specifically in the limit of $\omega_a = 0$, $g_c = g_{c0} = \sqrt{\omega_c E_F/3} \approx 0.58\sqrt{\omega_c E_F}$, in contrast to the $g_c \to 0$ of the Bose or spin system.

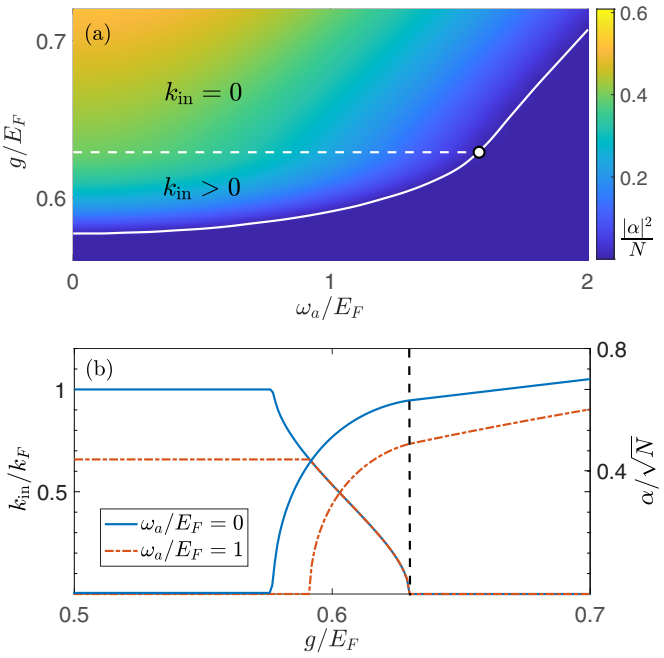

FIG. 1. (a) The solid line shows the critical atom-light coupling strength g_c/E_F as a function of atomic transition frequency ω_a/E_F. The color bar shows the scaled photon number $|\alpha|^2/N$. The dashed line separates the superradiant state with ($k_{\rm in} > 0$) or without ($k_{\rm in} = 0$) an inner Fermi surface, which ends at a tricritical point at $(\omega_a/E_F, g/E_F) = (1.577, 0.6288)$. (b) The Fermi momentum $k_{\rm in}/k_F$ of the inner Fermi sea and the scaled superradiant order parameter $\alpha/\sqrt{N}$ as functions of the atom-light coupling strength g/E_F for different $\omega_a/E_F = 0$ (blue solid) and 1 (red dash-dotted). Here, the light field frequency $\omega_c/E_F = 1$.

More remarkable in Fig. 1(a), we find a regime in which the superradiance can coexist with an (inner) Fermi sea. To see it clearly, in Fig. 1(b) we plot the evolution of the Fermi momentum $k_{\rm in}$ of the Fermi sea and the scaled superradiant order parameter $\alpha/\sqrt{N}$ with respect to the atom-light coupling g. One can see that for an intermediate-coupling strength g ($> g_c$), we have $\alpha \neq 0$ and $k_{\rm in} > 0$, suggesting a coexisting state with both superradiance and a normal Fermi sea. The emergence of a such state is a unique feature of this fermionic system and is distinct from the bosonic counterpart, which results from the interplay of the Fermi blocking and the atom-light coupling.

To understand the underlying physics, it is intuitive to first consider $\omega_a = 0$. In this case, the atoms form a (spinful) Fermi sea in the momentum space with Fermi momentum $k_{\rm F}$ of the Fermi surface for $g = 0$. To produce the superradiance, one needs to bring the atoms out of the Fermi sea to form the polaritons on top of the Fermi surface, which nevertheless is energetically unfavorable for $g < g_c$, with $k_{\rm in} = k_F$ and $\alpha = 0$ shown in Fig. 1(b). When the coupling strength g goes beyond the threshold g_c, the energy cost to take atoms out of the Fermi surface can be compensated by the formation of polaritons for the atoms around the Fermi surface, which generate the superradiance, while the atoms deep in the Fermi sea are not

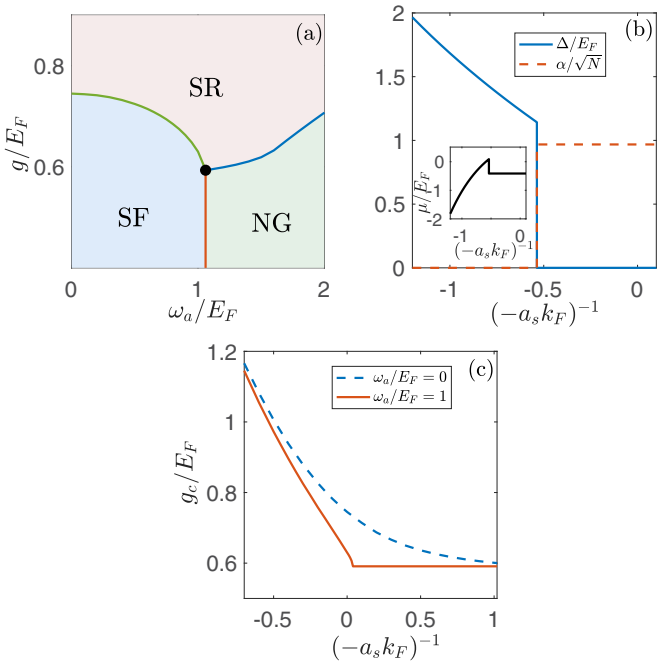

FIG. 2. (a) The ground-state phase diagram in the g-ω_a plane at unitary regime with $(-a_sk_F)^{-1}=0$, which contains three phases: the superfluid (SF) state, the superradiant (SR) state, and the normal gas (NG); (b) the SF order parameter Δ/E_F (blue solid) and the SR order parameter $\alpha/\sqrt{N}$ (red dash-dotted) as functions of scattering length $(-a_sk_F)^{-1}$. The inset shows the evolution of the chemical potential μ. Other parameters are $\omega_c/E_F=\omega_a/E_F=g/E_F=1$. (c) The critical coupling strength g_c/E_F as a function of the scattering length $(-a_sk_F)^{-1}$ for $\omega_a=0$ (blue dashed) and $\omega_a/E_F=1$ (red solid). Here $\omega_c/E_F=1$.

affected by the uniform atom-light coupling and form an inner Fermi sea with Fermi momentum $k_{\rm in}<k_F$, giving rise to the phase separation in momentum space. Further increasing g, more and more atoms contribute to the superradiance, and the inner Fermi surface is smeared out gradually with a decreasing $k_{\rm in}$ [see Fig. 1(b)]. Finally, across a second critical coupling $g_t=\sqrt{\omega_cE_F/2^{4/3}}\approx 0.63\sqrt{\omega_cE_F}$ (labeled by the dashed line in Fig. 1), all atoms are involved in the superradiance and $k_{\rm in}=0$. For $\omega_a>0$, the parameter regime of the superradiant state with an inner Fermi surface shrinks and vanishes at a tricritical point $\omega_a=2^{2/3}E_F\simeq 1.59E_F$ and $g_c=g_t$. In comparison, such a unique superradiant state is absent in 2D [51], where the constant density of states gives a constant superradiance threshold below $\omega_a/E_F=1$.

B. Interacting case

Above we have discussed the case without atomic interaction. When the atom-atom attraction is included, we solve Eqs. (11)– (13) to find the ground state. Figure 2(a) depicts the phase diagram in the g-ω_a plane, which contains three different phases: the SR, NG, and a superfluid (SF) state. For small g and ω_a, the system is always in a SF state with Bardeen-Cooper-Schrieffer (BCS) type pairing. For large ω_a, such BCS pairing is suppressed and the ground state becomes a polarized NG. With the increasing of g, both the SF and NG undergo a transition to the SR phase. The difference is that for the SF, the transition to SR is of first-order while it is continuous for the NG [refer to Fig. 2(b) and the corresponding discussions in the following]. These three phase transition lines merge at a tricritical point.

The discontinuous transition between the SF and SR states suggests that the two orders cannot coexist in the mean-field ground state [56]. In Fig. 2(b), we give a typical evolution of the order parameter Δ and α across the superradiant transition by tuning the scattering length. One can clearly see that in the SF phase, $\Delta\neq 0$ and $\alpha=0$, while $\alpha\neq 0$ and $\Delta=0$ for the SR state. It can be understood that the spin-flipping terms in the atom-light coupling, which behave like a transverse magnetic field and tend to form (triplet) polaritons, are in competition with the atomic singlet pairing from the contact interaction [24]. As a result, in the BEC regime ($a_s>0$), a larger g is required to break the tight binding between atoms compared with that required for the loose pairs in the BCS regime ($a_s<0$) [refer to Fig. 2(c)]. It is worth noting that unlike the suppression of superfluid in a large polarized environment, here the atom-light coupling itself does not introduce polarization (though it produces an effective Zeeman field), and it can destroy the singlet pairing even for $\omega_a=0$ with vanishing polarization.

Figure 2(c) presents the critical coupling strength g_c as a function of scattering length a_s for different ω_a. In general, g_c decreases with a_s moving from the BEC side to the BCS side, and it approaches the noninteracting result in the BCS limit. Note that for $\omega_a\neq 0$, g_c becomes a constant in the weak-coupling regime, where the ground state is a polarized NG independent of the scattering length.

C. Fluctuation spectrum

To further characterize the unique phases and phase transitions, we turn to the excitation spectrum of the fluctuations $\delta\Delta$ and $\delta\alpha$ around the mean-field ground state. From Eq. (8), the action of the fluctuation can be rewritten as

$$S_{\rm F}=-\frac{\beta V}{U}\sum_q\delta\bar{\Delta}_q\delta\Delta_q+\beta\sum_n\delta\bar{\alpha}_n(-i\nu_n+\omega_c)\delta\alpha_n+\sum_{k,q}\frac{1}{4}{\rm Tr}[\mathcal{G}_0(k)\mathcal{M}_F(-q)\mathcal{G}_0(k-q)\mathcal{M}_F(q)],\quad(17)$$

where $k=(\mathbf{k},i\omega_n)$ and $q=(\mathbf{q},i\nu_n)$, with $\nu_n=n\frac{2\pi}{\beta}$, $n\in Z$ being the bosonic Matsubara frequency. As Δ and α cannot coexist, the fluctuations $\delta\Delta$ and $\delta\alpha$ in Eq. (17) are decoupled, which for $\Delta=0$ takes the form of (see the Appendix for more details)

$$S_{\rm F}=\beta\sum_q\Xi_q\delta\bar{\Delta}_q\delta\Delta_q+\frac{\beta}{2}\sum_n(\delta\bar{\alpha}_n\quad\delta\alpha_n)\mathcal{G}_\alpha^{-1}\begin{pmatrix}\delta\alpha_n\\ \delta\bar{\alpha}_n\end{pmatrix}.\quad(18)$$

Here $\Xi_q=\sum_{\mathbf{k},s}\frac{1-n_f(E_{\mathbf{k},s})-n_f(E_{\mathbf{k}-\mathbf{q},s})}{i\nu_n-\xi_{\mathbf{k}}-\xi_{\mathbf{k}-\mathbf{q}}}-\frac{V}{U}$ describes the familiar spectrum of the pair fluctuation [55], and

$$\mathcal{G}_\alpha^{-1}=\begin{pmatrix}\mathcal{K}_1&\mathcal{K}_2\\ \mathcal{K}_2&\mathcal{K}_1\end{pmatrix},\quad(19)$$

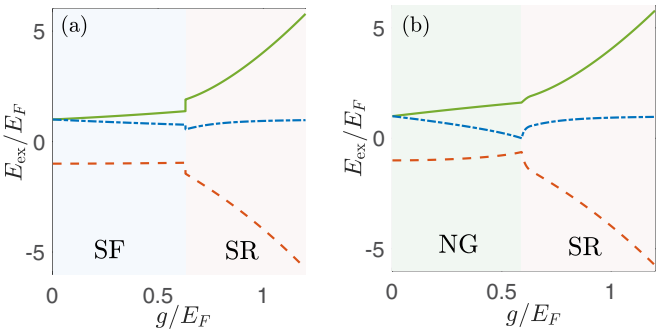

FIG. 3. Evolution of the excitation energy E_{ex}/E_F vs the atom-light coupling strength g/E_F for two typical interaction parameters: (a) $-1/a_s k_F = -1$ and (b) $-1/a_s k_F = 1$. Here, $\omega_c/E_F = \omega_a/E_F = 1$. There are three branches: one is of photon-type (blue dash-dotted) and two are of matter-type (green solid and red dashed).

$$\mathcal{K}_1 = -i\nu_n + \omega_c - \frac{g^2}{N}\sum_{\mathbf{k},s}\frac{s\omega_a^2 \tanh\left(\frac{\beta E_{\mathbf{k},s}}{2}\right)}{2\Lambda\left(\nu_n^2 + 4\Lambda^2\right)}, \tag{20}$$

$$\mathcal{K}_2 = -\frac{g^2}{N}\sum_{\mathbf{k},s}\frac{s\omega_a^2}{2\Lambda\left(\nu_n^2 + 4\Lambda^2\right)}\tanh\left(\frac{\beta E_{\mathbf{k},s}}{2}\right) \tag{21}$$

is the fluctuated Green function of the light field, with the pole of $\mathcal{G}_\alpha$ giving the excitation energy. For $\alpha = 0$, we can also derive the corresponding fluctuation action and the resultant excitation spectrum (see the Appendix for explicit expressions).

In this paper, we are interested in the unique excitations of the light field, which carry the information of the underlying many-body ground states not captured in the mean-field level and can be measured via the cavity transmission spectrum [57,58]. In Fig. 3, we plot the excitation spectrum E_{ex} as a function of atom-light coupling g for two typical scattering lengths. In general, there are three branches of E_{ex} contributed by the photon fluctuation via three types of excitations: one is of photon-type by simply creating or annihilating a single photon ($\sim\omega_c$, blue dashed-dotted line), and the other two are of matter-type by annihilating an $\downarrow$-atom and creating an $\uparrow$-atom ($\sim\omega_a$, green solid line) and vice versa ($\sim -\omega_a$, red dashed line), which are decoupled for $g = 0$. With the increase of g, such excitations couple to each other with the energy E_{ex} of each branch been corrected by the atom-light coupling.

Below the superradiant threshold g_c, one can see that the excitation spectrum is weakly dependent on g for a SF state [Fig. 3(a) with $(-a_s k_F)^{-1} = -1$] while it is considerably modified by g for a NG [Fig. 3(b) with $(-a_s k_F)^{-1} = 1$]. Above g_c, the excitations in the deep SR regime exhibit similar behaviors for both cases except around the critical point g_c, where the excitation energy E_{ex} exhibits a discontinuous jump for all branches across the SF-SR transition. In contrast for a NG, the single-photon excitation energy decreases with g continuously, and becomes zero at the superradiance transition point [see the blue dashed-dotted line in Fig. 3(b)]. We emphasize that the unique dependency of the excitation spectrum on relevant parameters in different phases can not only signal the (first-order) phase transitions, but it can also carry the important information of each phase, which is beyond the mean-field theory and can be accessible in experiment.

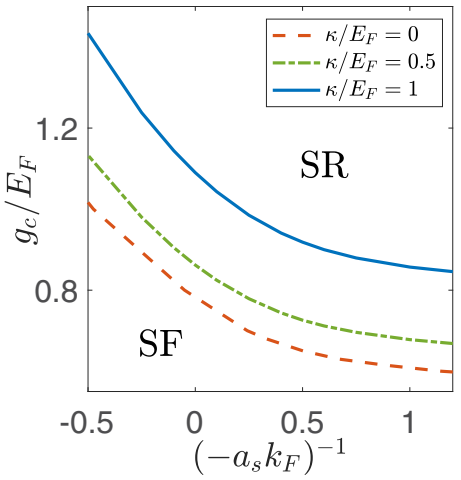

FIG. 4. The SR critical coupling strength g_c/E_F as a function of $(-a_s k_F)^{-1}$ for decay rate $\kappa = 0$ (red dashed), 0.5 (green dot-dashed), and 1 (blue solid). Here, $\omega_a = 0$ and $\omega_c/E_F = 1$.

IV. DISCUSSION AND CONCLUSION

So far, we have discussed the results of equilibrium states without decay. For a realistic cavity realization of the single-mode light field [53], one needs to take into account the loss of the cavity field due to the leakage, which can generally be captured by the master equation $\partial_t\rho = -i[\hat{H}, \rho] + \kappa(2\hat{\alpha}\rho\hat{\alpha} - \hat{\alpha}\hat{\alpha}^\dagger\rho - \rho\hat{\alpha}^\dagger\hat{\alpha})$ on the density matrix ρ, with κ being the decay rate. Instead, a nonequilibrium steady state can be expected [28], which is achieved by writing

$$i\partial_t\alpha = (\omega_c - i\kappa)\alpha + \frac{g}{\sqrt{N}}(R + R^*) \tag{22}$$

with $\alpha \equiv \langle\hat{\alpha}\rangle$ and $R \equiv \sum_{\mathbf{k}}\langle\hat{c}^\dagger_{\mathbf{k}\uparrow}\hat{c}_{\mathbf{k}\downarrow}\rangle$. For a steady state, $\partial_t\alpha = 0$ and we have

$$\alpha = -\frac{g(R + R^*)}{\sqrt{N}(\omega_c - i\kappa)}. \tag{23}$$

Solving the above Eq. (23) together with Eqs. (11) and (13) self-consistently, we can obtain the steady-state phase diagram, as shown in Fig. 4. Compared to the (equilibrium) case without decay ($\kappa = 0$), we find that the critical atom-light coupling strength g_c increases with κ, with a global shift of the phase boundary. This becomes transparent in the limit of weak interaction, where g_c can be derived explicitly as

$$g_c/E_F = \sqrt{\frac{\omega_c^2 + \kappa^2}{\omega_c}\frac{4E_F}{\omega_a^2 + 12\mu^2}}. \tag{24}$$

For $\kappa = 0$, it recovers the dissipationless result given by Eq. (16).

In Fig. 5, we plot the evolution of the excitation spectrum across the SF-SR/NG-SR transition in the presence of a finite κ. Compared to the case of $\kappa = 0$, an important consequence brought about by the cavity decay is that due to the atom-light coupling, all three branches become dissipated with a complex energy. For the real parts of the energy [Figs. 5(a) and

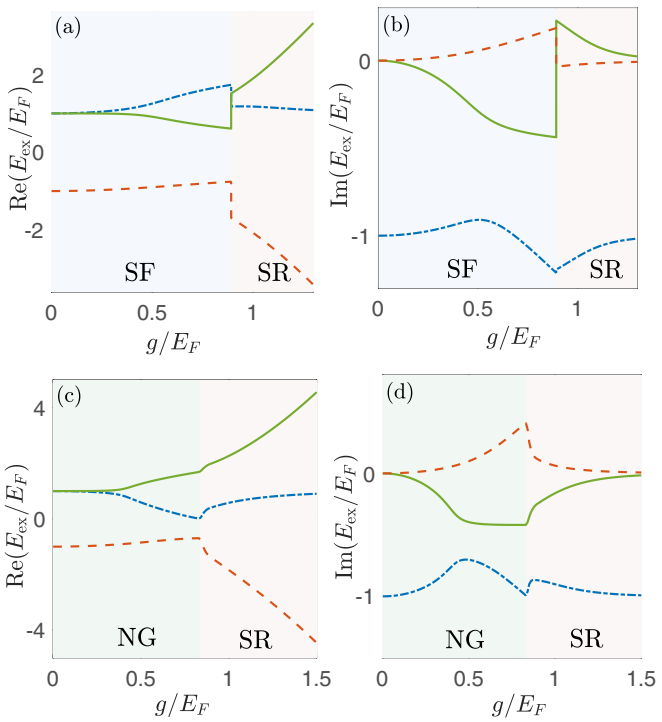

FIG. 5. The real part (a), (c) and the imaginary part (b), (d) of the excitation energy E_{ex}/E_F as functions of g/E_F for two interaction parameters: (a), (b) $-1/a_s k_F = 0$ and (c), (d) $-1/a_s k_F = 1$. Here, $\kappa/E_F = 1$ and other parameters are the same as in Fig. 3.

5(c)], they show similar behaviors to that of $\kappa = 0$ (Fig. 3), while for the imaginary part it approaches $-\kappa/E_F \sim -1$ in the NG phase with small g or in the SR phase with large g, and there is a considerable variation in the intermediate regime for the photon-type branch [blue dash-dotted lines in Figs. 5(b) and 5(d)]; on the other hand, for the two matter-type branches [green solid and red dashed lines in Figs. 5(b) and 5(d)], the imaginary parts vanish in the small/large g limit and become significant in the intermediate regime.

We have focused above on the BCS-type pairing of the Fermi gas. It is also possible to consider polarized superfluid phases such as the Sarma phase [59] and the Fulde-Ferrell-Larkin-Ovchinnikov (FFLO) state [60,61] in this system. However, on the mean-field level, such polarized superfluid phases still arise from the singlet pairing induced by the contact interaction, and thus they cannot coexist with the superradiance as the BCS-type superfluid discussed above. Moreover, since the Sarma state mainly appears at finite temperature while the FFLO state appears in a very narrow parameter regime in the phase diagram of a polarized Fermi gas [62], their contributions to the zero-temperature phase diagram are quite small, and are therefore neglected in this work.

In experiment, we note that the strong coupling between a Fermi gas and an optical cavity has been realized recently [53], where the low-lying (ground-state) energy level and the high-lying excited one of the ^{6}Li atom is directly coupled to an optical cavity mode. To realize the Dicke-type atom-light coupling, one may also resort to the cavity-assisted Raman transition between two hyperfine states [63]. The contact interaction strength can be tuned by Feshbach resonance [64], which enable us to address the whole phase diagram across the BEC-BCS crossover. To detect the superradiance transition, one can measure the photon number leaking from the cavity [1], and/or the (fluctuated) excitation spectrum. The latter is closely related to the optical absorption of the cavity [65], and it can be obtained via the transmission spectrum [57,58].

In summary, we have investigated the ground-state phase diagram and the excitation spectrum of an interacting Fermi gas coupled to a single-mode light field homogeneously. The competition between interatomic singlet pairing interaction and atom-light coupling can lead to a first-order transition between the SF and SR orders with a tricritical point in the phase diagram. Due to the Fermi blocking, a finite atom-light coupling strength is generally needed to induce the SR order even for a vanishing atomic transition frequency, in contrast to the Dicke transition of a bosonic or spin system. It would also be interesting to find more exotic states like the unconventional superradiant superfluid with both SR and SF orders simultaneously in this hybrid system, but this is beyond the scope of this work, and we leave it for future studies.

ACKNOWLEDGMENTS

This work is supported by the National Natural Science Foundation of China under Grants No. 11875195, No. 62175169, No. 12175027, and No. 11875010, and by the Natural Science Foundation of Chongqing under Grant No. cstc2019jcyj-msxmX0217.

APPENDIX: DERIVATION OF THE FLUCTUATION SPECTRUM

To evaluate the fluctuation action Eq. (17), we write the Green's function at the saddle point as

$$\mathcal{G}_0(k) = \frac{1}{\prod_{s=\pm}\left(\omega_n^2 + E_{\mathbf{k},s}^2\right)} \begin{pmatrix} \mathcal{G}_{0,11} & \mathcal{G}_{0,12} & 0 & \mathcal{G}_{0,14} \\ \mathcal{G}_{0,21} & \mathcal{G}_{0,22} & \mathcal{G}_{0,23} & 0 \\ 0 & \mathcal{G}_{0,32} & \mathcal{G}_{0,33} & \mathcal{G}_{0,34} \\ \mathcal{G}_{0,41} & 0 & \mathcal{G}_{0,34} & \mathcal{G}_{0,44} \end{pmatrix}, \tag{A1}$$

where

$$\mathcal{G}_{0,11} = \left(-i\omega_n + \xi_{\mathbf{k}} + \frac{\omega_a}{2}\right)\left[(-i\omega_n - \xi_{\mathbf{k}})^2 - \Lambda^2\right] - |\Delta_0|^2\left(-i\omega_n - \xi_{\mathbf{k}} - \frac{\omega_a}{2}\right), \tag{A2}$$

$$\mathcal{G}_{0,22} = \left(-i\omega_n + \xi_{\mathbf{k}} - \frac{\omega_a}{2}\right)\left[(-i\omega_n - \xi_{\mathbf{k}})^2 - \Lambda^2\right] - |\Delta_0|^2\left(-i\omega_n - \xi_{\mathbf{k}} + \frac{\omega_a}{2}\right), \tag{A3}$$

$$\mathcal{G}_{0,33} = \Big(-i\omega_n + \xi_{\mathbf{k}} - \frac{\omega_a}{2}\Big)[(-i\omega_n + \xi_{\mathbf{k}})^2 - \Lambda^2] - |\Delta_0|^2\Big(-i\omega_n + \xi_{\mathbf{k}} + \frac{\omega_a}{2}\Big), \tag{A4}$$

$$\mathcal{G}_{0,44} = \Big(-i\omega_n - \xi_{\mathbf{k}} + \frac{\omega_a}{2}\Big)[(-i\omega_n + \xi_{\mathbf{k}})^2 - \Lambda^2] - |\Delta_0|^2\Big(-i\omega_n + \xi_{\mathbf{k}} - \frac{\omega_a}{2}\Big), \tag{A5}$$

$$\mathcal{G}_{0,12} = \mathcal{G}^*_{0,21} = \frac{g(\bar{\alpha}_0 + \alpha_0)}{\sqrt{N}}\big[\big(-i\omega_n - \xi^2_{\mathbf{k}} - \Lambda\big)\big(-i\omega_n - \xi^2_{\mathbf{k}} + \Lambda\big) + |\Delta_0|^2\big], \tag{A6}$$

$$\mathcal{G}_{0,14} = \mathcal{G}^*_{0,41} = \bar{\Delta}_0\Big[\Big(-i\omega_n + \varepsilon_{\mathbf{k}} + \frac{\omega_a}{2}\Big)\Big(-i\omega_n - \varepsilon_{\mathbf{k}} + \frac{\omega_a}{2}\Big) + \frac{g^2(\bar{\alpha}_0 + \alpha_0)^2}{N}\Big], \tag{A7}$$

$$\mathcal{G}_{0,23} = \mathcal{G}^*_{0,32} = -\bar{\Delta}_0\Big[\Big(-i\omega_n - \varepsilon_{\mathbf{k}} - \frac{\omega_a}{2}\Big)\Big(-i\omega_n + \varepsilon_{\mathbf{k}} - \frac{\omega_a}{2}\Big) + \frac{g^2(\bar{\alpha}_0 + \alpha_0)^2}{N}\Big], \tag{A8}$$

$$\mathcal{G}_{0,34} = \mathcal{G}^*_{0,43} = -\frac{g(\bar{\alpha}_0 + \alpha_0)}{\sqrt{N}}\big[\big(-i\omega_n + \xi^2_{\mathbf{k}} + \Lambda\big)\big(-i\omega_n + \xi^2_{\mathbf{k}} - \Lambda\big) + |\Delta_0|^2\big]. \tag{A9}$$

As Δ and α cannot coexist in the mean-field ground state, i.e., $\Delta_0 = 0$ or $\alpha_0 = 0$, this would simplify the calculations, and in the following we present the results in those cases.

Case I: $\Delta_0 = 0$. In this case, the system can be a normal state ($\alpha = 0$) or a SR state ($\alpha \neq 0$). We have

$$\sum_{k,q}\frac{1}{4}\mathrm{Tr}[\mathcal{G}_0(k)\mathcal{M}_F(-q)\mathcal{G}_0(k-q)\mathcal{M}_F(q)] = \sum_n \frac{1}{2}\begin{pmatrix}\delta\overline{\alpha}_n & \delta\alpha_n\end{pmatrix}\begin{pmatrix}\mathcal{G}_{\bar{\alpha}\alpha} & \mathcal{G}_{\bar{\alpha}\bar{\alpha}}\\ \mathcal{G}_{\alpha\alpha} & \mathcal{G}_{\alpha\bar{\alpha}}\end{pmatrix}\begin{pmatrix}\delta\alpha_n\\ \delta\bar{\alpha}_n\end{pmatrix} + \sum_q \mathcal{G}_\Delta \delta\bar{\Delta}_q\delta\Delta_q, \tag{A10}$$

where

$$\begin{aligned}\mathcal{G}_{\bar{\alpha}\alpha} &= \mathcal{G}_{\alpha\bar{\alpha}} = \mathcal{G}_{\bar{\alpha}\bar{\alpha}} = \mathcal{G}_{\alpha\alpha}\\ &= \frac{g^2}{N}\sum_{k,\mathbf{q}}[\mathcal{G}_{0,12}(k)\mathcal{G}_{0,12}(k-q) + \mathcal{G}_{0,11}(k)\mathcal{G}_{0,22}(k-q) + \mathcal{G}_{0,34}(k)\mathcal{G}_{0,34}(k-q) + \mathcal{G}_{0,33}(k)\mathcal{G}_{0,44}(k-q)],\end{aligned} \tag{A11}$$

$$\mathcal{G}_\Delta = \sum_k[\mathcal{G}_{0,12}(k)\mathcal{G}_{0,34}(k-q) + \mathcal{G}_{0,11}(k)\mathcal{G}_{0,44}(k-q) + \mathcal{G}_{0,22}(k)\mathcal{G}_{0,33}(k-q) - \mathcal{G}_{0,21}(k)\mathcal{G}_{0,34}(k-q)]. \tag{A12}$$

Substituting Eqs. (A2)–(A9) into the above equations (A11) and (A12) and performing the summation over the Matsubara frequencies $i\omega_n$, we obtain

$$\frac{1}{\beta}\mathcal{G}_{\bar{\alpha}\alpha} = -\frac{g^2}{N}\sum_{\mathbf{k},s}\frac{s\omega_a^2}{2\Lambda\big(\nu_n^2 + 4\Lambda^2\big)}\tanh\frac{\beta E_{\mathbf{k},s}}{2}, \tag{A13}$$

$$\frac{1}{\beta}\mathcal{G}_\Delta = \sum_{\mathbf{k},s}\frac{1 - n_F(E_{\mathbf{k},s}) - n_F(E_{\mathbf{k}-\mathbf{q},s})}{i\nu_n - \xi_{\mathbf{k}} - \xi_{\mathbf{k}-\mathbf{q}}}. \tag{A14}$$

Here we have taken use of $\frac{1}{\beta}\sum_n \frac{1}{i\omega_n - \epsilon} = n_F(\epsilon)$ with the Fermi distribution function $n_F(\epsilon) = \frac{1}{\exp(\beta\epsilon)+1}$. Putting the free terms of the fluctuations together, we can derive the final form Eqs. (18)–(21) in the main text.

Case II: $\alpha_0 = 0$. In this case, the system can be a SF state ($\Delta \neq 0$) or a NG ($\Delta = 0$). Similar to case I, we can derive the final form of the fluctuation action Eq. (17), which is given by

$$S_F = \frac{1}{2}\Bigg[\sum_n \begin{pmatrix}\delta\overline{\alpha}_n & \delta\alpha_n\end{pmatrix}\begin{pmatrix}\mathcal{G}_{\bar{\alpha}\alpha} & \mathcal{G}_{\bar{\alpha}\bar{\alpha}}\\ \mathcal{G}_{\alpha\alpha} & \mathcal{G}_{\alpha\bar{\alpha}}\end{pmatrix}\begin{pmatrix}\delta\alpha_n\\ \delta\bar{\alpha}_n\end{pmatrix} + \sum_q \begin{pmatrix}\delta\overline{\Delta}_q & \delta\Delta_q\end{pmatrix}\begin{pmatrix}\mathcal{G}_{\bar{\Delta}\Delta} & \mathcal{G}_{\bar{\Delta}\bar{\Delta}}\\ \mathcal{G}_{\Delta\Delta} & \mathcal{G}_{\Delta\bar{\Delta}}\end{pmatrix}\begin{pmatrix}\delta\Delta_q\\ \delta\bar{\Delta}_q\end{pmatrix}\Bigg], \tag{A15}$$

where $\mathcal{G}_{\bar{\alpha}\alpha} = \mathcal{G}_{\alpha\bar{\alpha}} = -i\nu_n + \omega_c + \mathcal{G}_{\bar{\alpha}\bar{\alpha}}$ with

$$\mathcal{G}_{\bar{\alpha}\bar{\alpha}} = \mathcal{G}_{\alpha\alpha} = \sum_{\mathbf{k},s}\frac{-s}{2\big(\nu_n^2 + \omega_a^2\big)}\Bigg\{\omega_a\tanh\frac{\beta E_{\mathbf{k},s}}{2} + \frac{4E^2_{\mathbf{k},s}\xi_{\mathbf{k}}(i\nu_n + \omega_a) + 2\nu_n^2\varepsilon_{\mathbf{k}}(\omega_a + s\varepsilon_{\mathbf{k}}) + \nu_n^2\xi_{\mathbf{k}}(i\nu_n - 2sE_{\mathbf{k},s})}{\varepsilon_{\mathbf{k}}\big(\nu_n^2 + 4E^2_{\mathbf{k},s}\big)}\Bigg\} \tag{A16}$$

and

$$\mathcal{G}_{\bar{\Delta}\Delta} = \mathcal{G}_{\Delta\bar{\Delta}} = \sum_{\mathbf{k},s}\Bigg\{\frac{\Pi(\mathbf{k},\mathbf{k}-\mathbf{q})n_F(E_{\mathbf{k},s})}{\varepsilon_{\mathbf{k}}\Upsilon_{\mathbf{k}}} + \frac{\Pi(\mathbf{k}-\mathbf{q},\mathbf{k})n_F(E_{\mathbf{k}-\mathbf{q},s})}{\varepsilon_{\mathbf{k}-\mathbf{q}}\Upsilon_{\mathbf{k}}} + \frac{\mathcal{A}_{\mathbf{k}}}{2\varepsilon_{\mathbf{k}}\varepsilon_{\mathbf{k}-\mathbf{q}}\big[(i\nu_n + \varepsilon_{\mathbf{k}})^2 - \varepsilon^2_{\mathbf{k}-\mathbf{q}}\big]}\Bigg\} - \frac{U}{V}, \tag{A17}$$

$$\mathcal{G}_{\bar{\Delta}\bar{\Delta}} = \mathcal{G}_{\Delta\Delta} = -\sum_{\mathbf{k},s}\frac{\bar{\Delta}_0^2}{2\Upsilon_{\mathbf{k}}}\Bigg[\frac{\big(\nu_n^2 - \varepsilon^2_{\mathbf{k}} + \varepsilon^2_{\mathbf{k}-\mathbf{q}}\big)n_F(E_{\mathbf{k},s})}{\varepsilon_{\mathbf{k}}} + \frac{\big(\nu_n^2 + \varepsilon^2_{\mathbf{k}} - \varepsilon^2_{\mathbf{k}-\mathbf{q}}\big)n_F(E_{\mathbf{k}-\mathbf{q},s})}{\varepsilon_{\mathbf{k}-\mathbf{q}}} - \frac{\mathcal{B}_{\mathbf{k}}}{2\varepsilon_{\mathbf{k}}\varepsilon_{\mathbf{k}-\mathbf{q}}}\Bigg]. \tag{A18}$$

Here $\Upsilon_{\mathbf{k}} = [\nu_n^2 - (\varepsilon_{\mathbf{k}} + \varepsilon_{\mathbf{k}-\mathbf{q}})^2][\nu_n^2 - (\varepsilon_{\mathbf{k}} - \varepsilon_{\mathbf{k}-\mathbf{q}})^2]$ and

$$\Pi(\mathbf{k}_1, \mathbf{k}_2) = \left(\varepsilon_{\mathbf{k}_1}^2 + i\nu_n\xi_{\mathbf{k}_1}\right)\left(\nu_n^2 + \varepsilon_{\mathbf{k}_1}^2\right) + i\nu_n\left[\varepsilon_{\mathbf{k}_2}^2(\xi_{\mathbf{k}_1} - \varepsilon_{\mathbf{k}_1}) - 2\varepsilon_{\mathbf{k}_1}^2\xi_{\mathbf{k}_2}\right] + \xi_{\mathbf{k}}\xi_{\mathbf{k}-\mathbf{q}}\left(\nu_n^2 + \varepsilon_{\mathbf{k}_2}^2 - \varepsilon_{\mathbf{k}_1}^2\right), \tag{A19}$$

$$\mathcal{A}_{\mathbf{k}} = i\nu_n(\xi_{\mathbf{k}-\mathbf{q}}\varepsilon_{\mathbf{k}} + \varepsilon_{\mathbf{k}-\mathbf{q}}\xi_{\mathbf{k}}) + (\xi_{\mathbf{k}}\xi_{\mathbf{k}-\mathbf{q}} - \varepsilon_{\mathbf{k}}\varepsilon_{\mathbf{k}-\mathbf{q}})(\varepsilon_{\mathbf{k}} + \varepsilon_{\mathbf{k}-\mathbf{q}}) + 2\varepsilon_{\mathbf{k}}\varepsilon_{\mathbf{k}-\mathbf{q}}(\xi_{\mathbf{k}} - \xi_{\mathbf{k}-\mathbf{q}}), \tag{A20}$$

$$\mathcal{B}_{\mathbf{k}} = \varepsilon_{\mathbf{k}-\mathbf{q}}(i\nu_n - \varepsilon_{\mathbf{k}-\mathbf{q}})^2 + \varepsilon_{\mathbf{k}}(i\nu_n + \varepsilon_{\mathbf{k}})^2 - \varepsilon_{\mathbf{k}-\mathbf{q}}\varepsilon_{\mathbf{k}}^2 - \varepsilon_{\mathbf{k}}\varepsilon_{\mathbf{k}-\mathbf{q}}^2. \tag{A21}$$

Numerically solving the pole of $\mathcal{G}$, we obtain the excitation spectrum given in the main text.

[1] K. Baumann, C. Guerlin, F. Brennecke, and T. Esslinger, Dicke quantum phase transition with a superfluid gas in an optical cavity, Nature (London) **464**, 1301 (2010).

[2] R. H. Dicke, Coherence in spontaneous radiation processes, Phys. Rev. **93**, 99 (1954).

[3] Y. K. Wang and F. T. Hioe, Phase transition in the Dicke model of superradiance, Phys. Rev. A **7**, 831 (1973).

[4] K. Hepp and E. H. Lieb, On the superradiant phase transition for molecules in a quantized radiation field: the dicke maser model, Ann. Phys. **76**, 360 (1973).

[5] K. Hepp and E. H. Lieb, Equilibrium statistical mechanics of matter interacting with the quantized radiation field, Phys. Rev. A **8**, 2517 (1973).

[6] D. Nagy, G. Szirmai, and P. Domokos, Self-organization of a Bose-Einstein condensate in an optical cavity, Eur. Phys. J. D **48**, 127 (2008).

[7] D. Nagy, G. Kónya, G. Szirmai, and P. Domokos, Dicke-Model Phase Transition in the Quantum Motion of a Bose-Einstein Condensate in an Optical Cavity, Phys. Rev. Lett. **104**, 130401 (2010).

[8] J. Keeling, M. J. Bhaseen, and B. D. Simons, Collective Dynamics of Bose-Einstein Condensates in Optical Cavities, Phys. Rev. Lett. **105**, 043001 (2010).

[9] H. Ritsch, P. Domokos, F. Brennecke, and T. Esslinger, Cold atoms in cavity-generated dynamical optical potentials, Rev. Mod. Phys. **85**, 553 (2013).

[10] H. Keßler, J. Klinder, M. Wolke, and A. Hemmerich, Steering Matter Wave Superradiance with an Ultranarrow-Band Optical Cavity, Phys. Rev. Lett. **113**, 070404 (2014).

[11] J. Keeling, M. Bhaseen, and B. Simons, Fermionic Superradiance in a Transversely Pumped Optical Cavity, Phys. Rev. Lett. **112**, 143002 (2014).

[12] F. Piazza and P. Strack, Umklapp Superradiance with a Collisionless Quantum Degenerate Fermi Gas, Phys. Rev. Lett. **112**, 143003 (2014).

[13] Y. Chen, Z. Yu, and H. Zhai, Superradiance of Degenerate Fermi Gases in a Cavity, Phys. Rev. Lett. **112**, 143004 (2014).

[14] Y. Chen, H. Zhai, and Z. Yu, Superradiant phase transition of Fermi gases in a cavity across a Feshbach resonance, Phys. Rev. A **91**, 021602(R) (2015).

[15] L. Zhou, H. Pu, K. Zhang, X.-D. Zhao, and W. Zhang, Cavity-induced switching between localized and extended states in a noninteracting Bose-Einstein condensate, Phys. Rev. A **84**, 043606 (2011).

[16] K. Rojan, R. Kraus, T. Fogarty, H. Habibian, A. Minguzzi, and G. Morigi, Localization transition in the presence of cavity backaction, Phys. Rev. A **94**, 013839 (2016).

[17] W. Zheng and N. R. Cooper, Anomalous diffusion in a dynamical optical lattice, Phys. Rev. A **97**, 021601(R) (2018).

[18] H. Yin, J. Hu, A.-C. Ji, G. Jūzeliunas, X.-J. Liu, and Q. Sun, Localization Driven Superradiant Instability, Phys. Rev. Lett. **124**, 113601 (2020).

[19] J. Klinder, H. Keßler, M. Reza Bakhtiari, M. Thorwart, and A. Hemmerich, Observation of a Superradiant Mott Insulator in the Dicke-Hubbard Model, Phys. Rev. Lett. **115**, 230403 (2015).

[20] R. Landig, L. Hruby, N. Dogra, M. Landini, R. Mottl, T. Donner, and T. Esslinger, Quantum phases from competing short- and long-range interactions in an optical lattice, Nature (London) **532**, 476 (2016).

[21] J. Léonard, A. Morales, P. Zupancic, T. Esslinger, and T. Donner, Supersolid formation in a quantum gas breaking a continuous translational symmetry, Nature (London) **543**, 87 (2017).

[22] J. Léonard, A. Morales, P. Zupancic, T. Donner, and T. Esslinger, Monitoring and manipulating Higgs and Goldstone modes in a supersolid quantum gas, Science **358**, 1415 (2017).

[23] Z. Wu, Y. Chen, and H. Zhai, Emergent symmetry at superradiance transition of a Bose condensate in two crossed beam cavities, Sci. Bull. **63**, 542 (2018).

[24] Q. Sun, J. Hu, L. Wen, H. Pu, and A.-C Ji, Unbound-to-bound transition of two-atom polaritons in an optical cavity, Phys. Rev. A **98**, 033801 (2018).

[25] S. Ostermann, W. Niedenzu, and H. Ritsch, Unraveling the Quantum Nature of Atomic Self-Ordering in a Ring Cavity, Phys. Rev. Lett. **124**, 033601 (2020).

[26] C. Halati, A. Sheikhan, H. Ritsch, and C. Kollath, Numerically Exact Treatment of Many-Body Self-Organization in a Cavity, Phys. Rev. Lett. **125**, 093604 (2020).

[27] F. Mivehvara, F. Piazza, T. Donner, and H. Ritsch, Cavity QED with quantum gases: New paradigms in many-body physics, Adv. Phys. **70**, 1 (2021).

[28] F. Dimer, B. Estienne, A. S. Parkins, and H. J. Carmichael, Proposed realization of the Dicke-model quantum phase transition in an optical cavity QED system, Phys. Rev. A **75**, 013804 (2007).

[29] M. Landini, N. Dogra, K. Kroeger, L. Hruby, T. Donner, and T. Esslinger, Formation of a Spin Texture in a Quantum Gas Coupled to a Cavity, Phys. Rev. Lett. **120**, 223602 (2018).

[30] R. M. Kroeze, Y. Guo, V. D. Vaidya, J. Keeling, and B. L. Lev, Spinor Self-Ordering of a Quantum Gas in a Cavity, Phys. Rev. Lett. **121**, 163601 (2018).

[31] F. Mivehvar, F. Piazza, and H. Ritsch, Disorder-Driven Density and Spin Self-Ordering of a Bose-Einstein Condensate in a Cavity, Phys. Rev. Lett. **119**, 063602 (2017).

[32] E. J. Davis, G. Bentsen, L. Homeier, T. Li, and M. H. Schleier-Smith, Photon-Mediated Spin-Exchange Dynamics of Spin-1 Atoms, Phys. Rev. Lett. **122**, 010405 (2019).

[33] E. I. R. Chiacchio and A. Nunnenkamp, Dissipation-Induced Instabilities of a Spinor Bose-Einstein Condensate Inside an Optical Cavity, Phys. Rev. Lett. **122**, 193605 (2019).

[34] B. Buča and D. Jaksch, Dissipation Induced Nonstationarity in a Quantum Gas, Phys. Rev. Lett. **123**, 260401 (2019).

[35] A. Camacho-Guardian, R. Paredes, and S. F. Caballero-Benítez, Quantum simulation of competing orders with fermions in quantum optical lattices, Phys. Rev. A **96**, 051602(R) (2017).

[36] F. Schlawin and D. Jaksch, Cavity-Mediated Unconventional Pairing in Ultracold Fermionic Atoms, Phys. Rev. Lett. **123**, 133601 (2019).

[37] Z. Zheng and Z. D. Wang, Cavity-induced Fulde-Ferrell-Larkin-Ovchinnikov superfluids of ultracold Fermi gases, Phys. Rev. A **101**, 023612 (2020).

[38] F. Mivehvar and D. L. Feder, Synthetic spin-orbit interactions and magnetic fields in ring-cavity QED, Phys. Rev. A **89**, 013803 (2014).

[39] Y. Deng, J. Cheng, H. Jing, and S. Yi, Bose-Einstein Condensates with Cavity-Mediated Spin-Orbit Coupling, Phys. Rev. Lett. **112**, 143007 (2014).

[40] L. Dong, L. Zhou, B. Wu, B. Ramachandhran, and H. Pu, Cavity-assisted dynamical spin-orbit coupling in cold atoms, Phys. Rev. A **89**, 011602(R) (2014).

[41] L. Dong, C. Zhu, and H. Pu, Photon-induced spin-orbit coupling in ultracold atoms inside optical cavity, Atoms **3**, 182 (2015).

[42] F. Mivehvar and D. L. Feder, Enhanced stripe phases in spin-orbit-coupled Bose-Einstein condensates in ring cavities, Phys. Rev. A **92**, 023611 (2015).

[43] J.-S. Pan, X.-J. Liu, W. Zhang, W. Yi, and G.-C. Guo, Topological Superradiant States in a Degenerate Fermi Gas, Phys. Rev. Lett. **115**, 045303 (2015).

[44] C. Zhu, L. Dong, and H. Pu, Effects of spin-orbit coupling on Jaynes-Cummings and Tavis-Cummings models, Phys. Rev. A **94**, 053621 (2016).

[45] D. Yu, J.-S. Pan, X.-J. Liu, W. Zhang, and W. Yi, Topological superradiant state in Fermi gases with cavity induced spin-orbit coupling, Front. Phys. **13**, 136701 (2018).

[46] C. Halati, A. Sheikhan, and C. Kollath, Cavity-Induced Spin-Orbit Coupling in an Interacting Bosonic Wire, Phys. Rev. A **99**, 033604 (2019).

[47] R. M. Kroeze, Y. Guo, and B. L. Lev, Dynamical Spin-Orbit Coupling of a Quantum Gas, Phys. Rev. Lett. **123**, 160404 (2019).

[48] S. Ostermann, H. Ritsch, and F. Mivehvar, Many-body phases of a planar Bose-Einstein condensate with cavity-induced spin-orbit coupling, Phys. Rev. A **103**, 023302 (2021).

[49] J. Fan, X. Zhou, W. Zheng, W. Yi, G. Chen, and S. Jia, Magnetic order in a Fermi gas induced by cavity-field fluctuations, Phys. Rev. A **98**, 043613 (2018).

[50] E. Colella, S. Ostermann, W. Niedenzu, F. Mivehvar, and H. Ritsch, Antiferromagnetic self-ordering of a Fermi gas in a ring cavity, New J. Phys. **21**, 043019 (2019).

[51] Y. Feng, K. Zhang, J. Fan1, F. Mei, G. Chen, and S. Jia, Quantum mixed phases of a two dimensional polarized degenerate Fermi gas in an optical cavity, Sci. Rep. **7**, 10568 (2017).

[52] E. Colella, R. Citro, M. Barsanti, D. Rossini, and M.-L. Chiofalo, Quantum phases of spinful Fermi gases in optical cavities, Phys. Rev. B **97**, 134502 (2018).

[53] K. Roux, H. Konishi, V. Helson, and J. Brantut, Strongly correlated fermions strongly coupled to light, Nat. Commun. **11**, 2974 (2020).

[54] A. Dodel, A. Pikovski, I. Ermakov, M. Narozniak, V. Ivannikov, H. Wu, and T. Byrnes, Cooper pair polaritons in cold fermionic atoms within a cavity, Phys. Rev. Res. **2**, 013184 (2020).

[55] A. Altland and B. Simons, *Condensed Matter Field Theory*, 2nd ed. (Cambridge University Press, Cambridge, 2010), p. 786.

[56] At finite temperature, we can solve a coexistent solution with $\Delta \neq 0$ and $\alpha \neq 0$, which, however, is energetically unfavorable.

[57] F. Brennecke, T. Donner, S. Ritter, T. Bourdel, M. Köhl, and T. Esslinger, Cavity QED with a Bose-Einstein condensate, Nature (London) **450**, 268 (2007).

[58] Y. Colombe, T. Steinmetz, G. Dubois, F. Linke, D. Hunger, and J. Reichel, Strong atom-field coupling for Bose-Einstein condensates in an optical cavity on a chip, Nature (London) **450**, 272 (2007).

[59] G. Sarma, On the influence of a uniform exchange field acting on the spins of the conduction electrons in a superconductor, J. Phys. Chem. Solids **24**, 1029 (1963).

[60] P. Fulde and R. A. Ferrell, Superconductivity in a strong spin-exchange field, Phys. Rev. **135**, A550 (1964).

[61] A. I. Larkin and Y. N. Ovchinnikov, Nonuniform state in superconductors, Zh. Eksp. Teor. Fiz. **47**, 1136 (1964) [Sov. Phys. JETP **20**, 762 (1965)].

[62] K. B. Gubbels and H. T. C. Stoof, Imbalanced Fermi gases at unitarity, Phys. Rep. **525**, 255 (2013).

[63] Z. Zhang, C. H. Lee, R. Kumar, K. J. Arnold, S. J. Masson, A. L. Grimsmo, A. S. Parkins, and M. D. Barrett, Dicke-model simulation via cavity-assisted Raman transitions, Phys. Rev. A **97**, 043858 (2018).

[64] C. Chin, R. Grimm, P. Julienne, and E. Tiesinga, Feshbach resonances in ultracold gases, Rev. Mod. Phys. **82**, 1225 (2010).

[65] P. R. Eastham and P. B. Littlewood, Bose condensation of cavity polaritons beyond the linear regime: The thermal equilibrium of a model microcavity, Phys. Rev. B **64**, 235101 (2001).